JOURNAL OF MATERIALS SCIENCE 23 (1988) 3782–3791

Fracture of hot-pressed alumina and SiC-whisker-reinforced alumina composite

R. K. GOVILA
Materials Engineering Department, Scientific Research Laboratory, Ford Motor Company, PO Box 2053, Dearborn, Michigan 48121, USA

The flexural strength of hot-pressed alumina and SiC-whisker-reinforced alumina composite were evaluated as a function of temperature (20 to 1400° C in air environment), applied stress and time. Two mechanistic regimes were manifest in the temperature dependence of the fracture stress. A temperature-independent region of fast fracture (catastrophic crack extension) existed up to 800° C, in which the failure mode was a mixture of transgranular and intergranular crack propagation. In this region, the alumina composite showed significantly higher fracture strength and toughness compared to polycrystalline alumina. Above 800° C, both materials (alumina and alumina composite) displayed a decreasing fracture strength due to the presence of subcritical or slow crack growth which occurred intergranularly. Flexural stress rupture evaluation in the temperature range 600 to 1200° C has identified the stress levels for time-dependent and time-independent failures.

1. Introduction

The use of ceramic materials for structural high-temperature engineering components is being investigated for a number of applications, in particular, heat engines such as the gas turbine and diesel, and in wear mode applications such as cutting tool inserts. The primary reasons for their use in heat engines are good oxidation and thermal shock resistance, low coefficient of thermal expansion and retention of high strength up to 1000° C. There are at least two unusual characteristics with respect to the strength of brittle ceramics. The first is that the material is in ductile (macroscopically) and its strength is controlled by the largest inherent microcrack or flaw in a given stress field; also because there is typically a distribution of such flaws, there is a resulting scatter in material strength. The second is that inherent flaws due to processing and fabrication within the material can exhibit the phenomenon of slow (subcritical) crack growth (SCG) under load at high temperatures ($\geqslant$ 1000° C), suggesting that the strength is time dependent. As a result, one of the most critical factors in the structural application of ceramics is the ability to predict the reliability of a ceramic component for a given time (period). Therefore, before the ceramic material can be used in any commercial application, its reliability and durability must be established. This usually requires long-term testing (200 to 1000 h per specimen) as a function of temperature, applied stress and environment. The mechanical reliability and durability of a ceramic material can be considerably improved if fracture strength and toughness are increased. This principle has long been used (over 30 years) successfully in metals and polymer composite materials by incorporating fibres, whiskers or particulate dispersions in the matrix material. The same principle has been applied to ceramic–ceramic composite materials as reviewed by Donald and McMillan [1]. Recently, SiC whiskers have been used in reinforcing alumina matrix [2–5] and thereby improving significantly the fracture strength and toughness of polycrystalline alumina. It is believed that the increased toughness of the composite material is a result of crack arrest or deflection and whisker pull-out.

The present study was undertaken to characterize the strength behaviour of a commercially available alumina composite containing 15 wt % SiC whiskers and polycrystalline alumina (without SiC whiskers) by evaluating fracture strength as a function of temperature (20 to 1400° C); failure sites and the mode of crack propagation were examined fractographically. In addition, long-term durability and reliability were characterized using detailed flexural stress rupture testing at several temperatures.

2. Materials, specimen preparation and testing

2.1. Materials

The materials used in this study were polycrystalline alumina and an alumina composite containing 15 wt % SiC whiskers. Both materials were in the hot-pressed condition and supplied by Arco Chemical Company (now Advanced Composite Materials Corp.) Greer, S.C. The alumina grains ranged in size from 1 to 5 μm and the SiC whiskers were typically 0.2 to 0.4 μm in diameter and 3 to 8 μm long. The exact composition of alumina and alumina compositie, and hot-pressing parameters (time, temperature, pressure and environment) are not known due to the proprietary nature of these materials. However, it is believed that both materials contained small amounts of MgO ($\leqslant$ 0.5 wt %)

0022–2461/88 $03.00 + .12

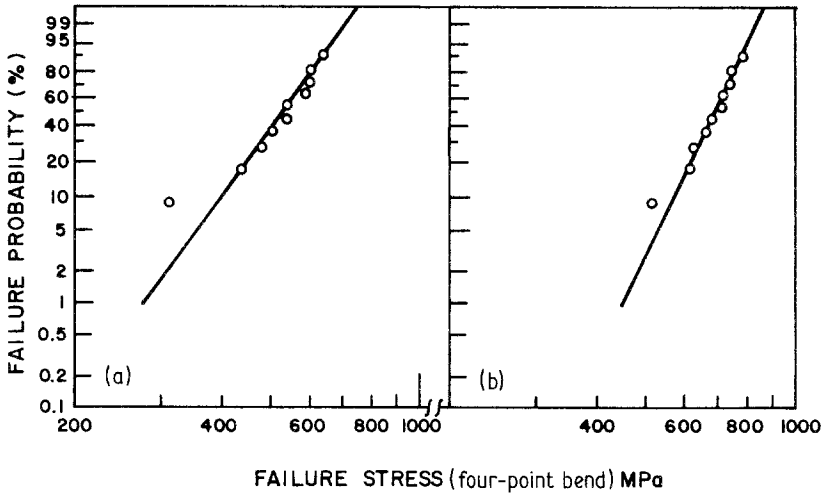

Figure 1 Statistical variation in fracture strength at 20° C for polycrystalline alumina and SiC-whisker-reinforced alumina composite. (a) 100% alumina, σ_{aug} = 521 MPa, σ_θ = 556 MPa, S.D. = 92 MPa, m = 6.6. (b) Alumina composite (85 wt % alumina + 15 wt % SiC whiskers), σ_{aug} = 676 MPa, σ_θ = 707 MPa, S.D. = 80 MPa, m = 10.

and Y_2O_3 ($\leqslant$ 2 wt %) to improve densification in hot-pressing. The polycrystalline alumina in the as-processed condition was off-white in colour while the alumina composite was dark green.

2.2. Specimen preparation and testing (fast fracture and stress rupture)

Flexural test specimens (approximately 32 mm long × 6 mm wide × 3 mm thick) were machined from the billets of material such that the tensile face was perpendicular to the hot-pressing direction, i.e. the strong direction [6]. All faces were ground lengthwise using 320 grit diamond wheels, and the edges were chamfered to prevent edge (localized stress concentration) effects. Complete details for flexural strength evaluation (in a fast fracture mode) at room temperature and above (600 to 1400° C), flexural stress rupture testing at elevated temperatures (600 to 1200° C) in air environment, self-aligning ceramic test fixture and test-span dimensions have been reported previously [6–8].

3. Results and discussion

3.1. Flexural strength and its variation with temperature

At room temperature, ten specimens each from two different materials, alumina and alumina composite, were tested in four-point bending to determine the fast fracture strength. Typical statistical variation in fracture strength, σ_F, at 20° C for polycrystalline alumina and SiC-whisker-reinforced alumina composite is shown in Fig. 1. For alumina, the σ_F varied from a minimum of 311 MPa to a maximum of 631 MPa with an average strength of 521 MPa, Weibull modulus of 6.6 and a standard deviation of 92 MPa. For alumina composite, the σ_F varied from a minimum of 514 MPa to a maximum of 779 MPa with an average strength of 676 MPa, Weibull modulus of 10 and a standard deviation of 80 MPa. Comparison of the σ_F values obtained at 20° C for the two materials indicates that the SiC-whisker-reinforced alumina composite is significantly stronger than the polycrystalline alumina. This increase in σ_F as displayed by the alumina

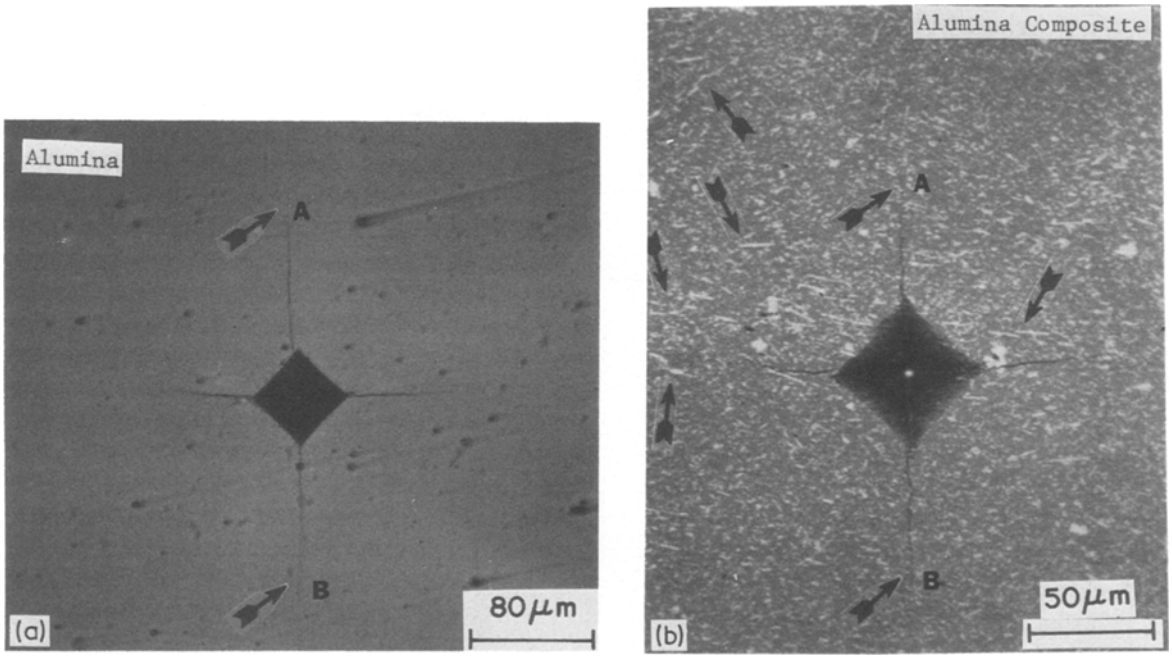

Figure 2 Optical micrographs showing controlled crack nucleation using a 4000 g load microhardness indentation on polished surfaces of test specimens. Small arrows in (b) indicate the presence of whiskers.

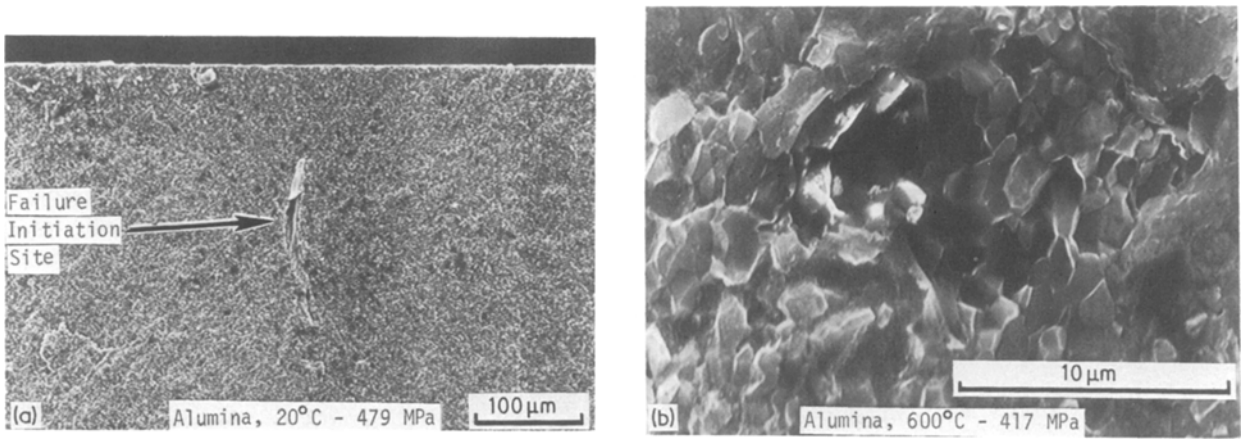

Figure 3 Typical SEM fractographs showing failure initiation sites in polycrystalline alumina specimens tested in fast fracture mode (machine cross-head speed = 0.5 mm min^{-1}).

composite is believed primarily due to the presence of SiC whiskers in the matrix which are significantly stronger than the individual alumina grains and thereby increasing the fracture strength of the matrix material. In addition, the SiC whiskers appear to offer greater resistance to crack propagation, probably due to crack deflection and resulting in higher fracture toughness. The above hypothesis was confirmed by making simple microhardness indentations on the polished surfaces of alumina and alumina composite, Fig. 2, and measuring the fracture toughness [9] from surface crack length using a 4000 g indenter load. Note the significantly increased length of the crack AB (Fig 2a) for the same load of indentation in alumina compared to alumina composite (Fig. 2b) which immediately suggests increased resistance to crack propagation in the composite material. Approximate fracture toughness values for alumina and alumina composite were 2.1 and 4.2 MPa m$^{0.5}$, respectively, at 20° C, and in agreement with measurements made by others [5].

Examination of the fracture surfaces of polycrystalline alumina specimens tested at 20° C revealed the presence of an "agglomerate or zone" of large-grained alumina grains as the failure initiating source. Typical examples of failure occurring at 20 and 600° C are shown in Figs 3a and b, respectively. The dark black spots surrounding the failure origin, Fig. 3a, are large grains of alumina distributed in a fine-grained alumina matrix. A similar type of failure initiating site was also observed in the alumina composite. In addition, the composite material showed failure initiation occurring at a large pore (20 to 40 μm diameter), surrounded by a "nest" or "haystack" of whiskers, Fig. 4. The presence of whiskers in a "nest" form suggests segregation occurring at an inhomogeneity and non-uniform distribution of whiskers in the matrix.

Flexural strength was also evaluated at higher temperatures (600 to 1400° C) and the variation in strength as a function of temperature for both materials is shown in Fig. 5. Complete strength data

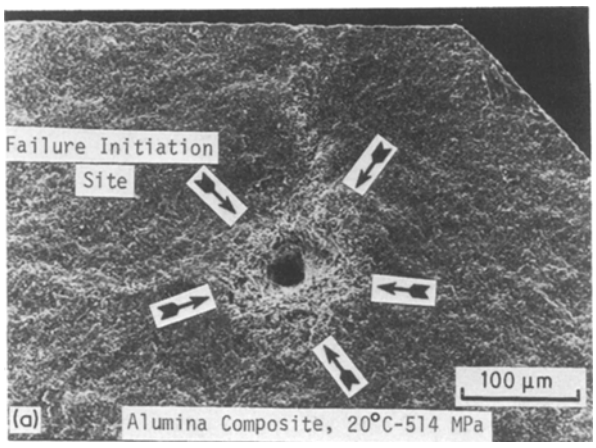

Figure 4 Typical failure site seen in SEM for an alumina composite specimen tested in fast fracture mode.

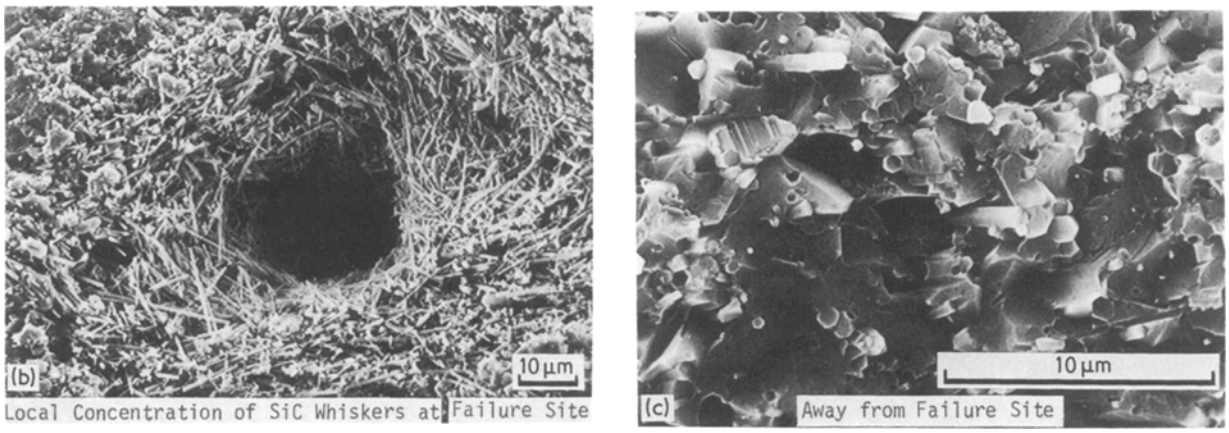

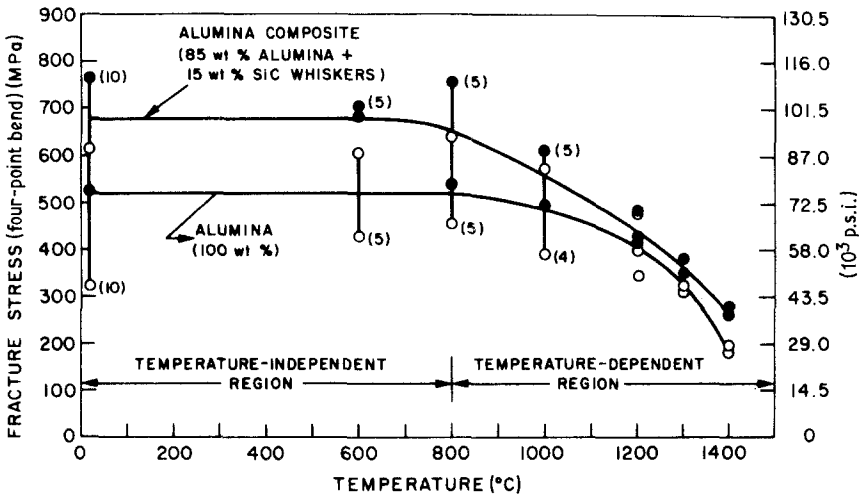

Figure 5 Variation in fast fracture strength as a function of temperature. Complete strength data are given in Tables I and II.

and the failure sources for alumina and alumina composite are given in Tables I and II, respectively. Both materials showed significant scatter in σ_F from 20 to 1000° C, Fig. 5, possibly due to variations in flaw size. At higher temperatures, especially in the range 1200 to 1400° C, both materials showed significantly decreased scatter in σ_F suggesting that fracture was governed by a different mechanism relative to fracture occurring in the temperature-independent region. For both materials, σ_F can be considered independent of temperature up to about 800° C. The constancy of σ_F in this temperature range implies that a single fracture mechanism predominates, and that insignificant plastic deformation (viscous flow due to glass formation) accompanied the fracture process. From the fractographs (Figs 3 and 4) it appears that the large alumina grains failed transgranularly and the fine-grained material displayed intergranular crack propagation, and as such the primary mode of crack propagation during fast fracture (catastrophic failure) could be

TABLE I Fast fracture strength data for hot-pressed alumina (100% alumina)

Test no.	Test temp. (° C)	Fracture strength (MPa)	Failure origin
1	20	597	Surface flaw
2		435	Corner failure
3		500	Surface flaw
4		536	Surface flaw
5		479	Sub-surface flaw, Fig. 3
6		597	Surface flaw
7		538	Surface flaw
8		631	Surface flaw
9		584	Surface flaw
10		311	Corner failure
11	600	472	Surface flaw
12		527	Surface flaw
13		608	Sub-surface flaw
14		619	Sub-surface flaw
15		417	Corner failure, Fig. 3
16	800	650	Sub-surface flaw
17		445	Sub-surface flaw
18		494	Surface flaw
19		632	Surface flaw
20		595	Surface flaw
21	1000	494	Surface flaw
22		379	Corner failure
23		586	Sub-surface flaw
24		483	Sub-surface flaw
25	1200	346	Surface flaw, Fig. 9
26		479	Sub-surface flaw, Fig. 10
27		400	Sub-surface flaw
28	1300	320	Sub-surface flaw, Fig. 11
29		312	Surface flaw
30	1400	182	Surface flaw
31		195	Sub-surface flaw

The as-processed material was off-white in colour.

TABLE II Fast fracture strength data for hot-pressed alumina composite (85% alumina + 15% silicon carbide whiskers)

Test no.	Test temp. (° C)	Fracture strength (MPa)	Failure origin
1	20	708	Surface flaw
2		623	Surface flaw
3		713	Sub-surface flaw
4		659	Surface flaw
5		674	Surface flaw
6		735	Sub-surface flaw
7		779	Surface flaw
8		514	Sub-surface flaw, Fig. 4
9		742	Surface flaw
10		612	Sub-surface flaw
11	600	670	Sub-surface flaw
12		702	Surface flaw
13		689	Surface flaw
14		718	Surface flaw
15		680	Sub-surface flaw
16	800	760	Surface flaw
17		527	Sub-surface flaw
18		768	Surface flaw
19		685	Surface flaw
20		656	Sub-surface flaw
21	1000	487	Sub-surface flaw, Fig. 6
22		571	Sub-surface flaw
23		626	Surface flaw
24		626	Sub-surface flaw
25		582	Sub-surface flaw
26	1200	428	Surface flaw
27		479	Surface flaw
28		417	Surface flaw
29	1300	347	Corner failure
30		378	Surface flaw
31	1400	263	SCG and creep, Fig. 8
32		277	SCG and creep

The as-processed material was dark green in colour.
SCG = slow crack growth.

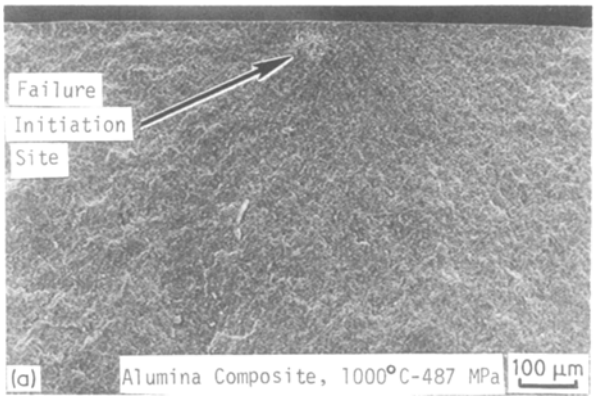

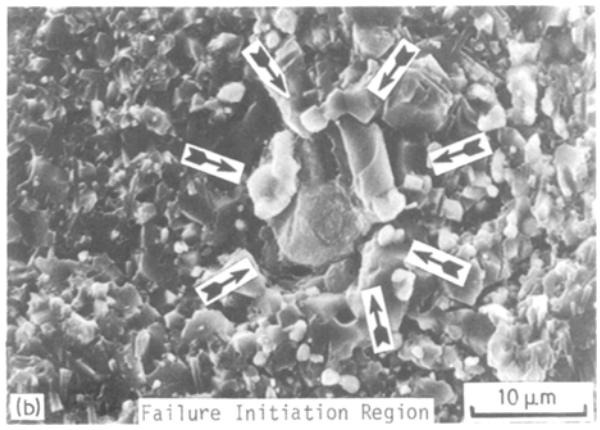

Figure 6 SEM fractographs showing failure initiation at a subsurface flaw.

classified as a mixture. A small decrease in σ_F was noted at 1000° C for the alumina composite while the polycrystalline alumina showed a less severe effect, Fig. 5. A typical fracture surface showing failure occurring at a local region of large alumina grains is shown in Fig. 6. Note the surrounding matrix material consisted of "fine-grained alumina" and SiC-whiskers. The distribution and dispersion of SiC-whiskers is clearly revealed in a region away from the failure origin, Fig. 6c. The fine porosity in the alumina matrix, micro-cracking around the large alumina grains, and whisker pull-out are visible on the fracture surface, Figs 5b and c.

The SiC-whisker-reinforced alumina composite showed a significant decrease in σ_F in tests made at 1200° C and above, Fig. 5, relative to σ_F in the temperature-independent region. The fracture surfaces at 1200 and 1300° C did not show the presence of the glassy phase or the occurrence of SCG possibly due to the nature of testing (fast fracture). It is believed that the decrease in strength, σ_F, in this temperature region (1200 to 1400° C) was considerably influenced by the presence of the glassy phase as confirmed by the stress rupture tests (see later). Up to 1300° C, the load–deflection or time curves showed linear elastic behaviour, and at 1400° C significant deviation from the elastic line was observed, indicative of creep deformation, Fig. 7. Examination of the fracture surface showed a localized SCG region as the failure zone, Fig. 8. The SCG region is distinct in its appearence, being characterized by a rough surface. The mode of fracture during SCG is primarily intergranular as indicated by grain separation and cavity formation, Fig. 8b, and outside the SCG region, it is a mixture of transgranular

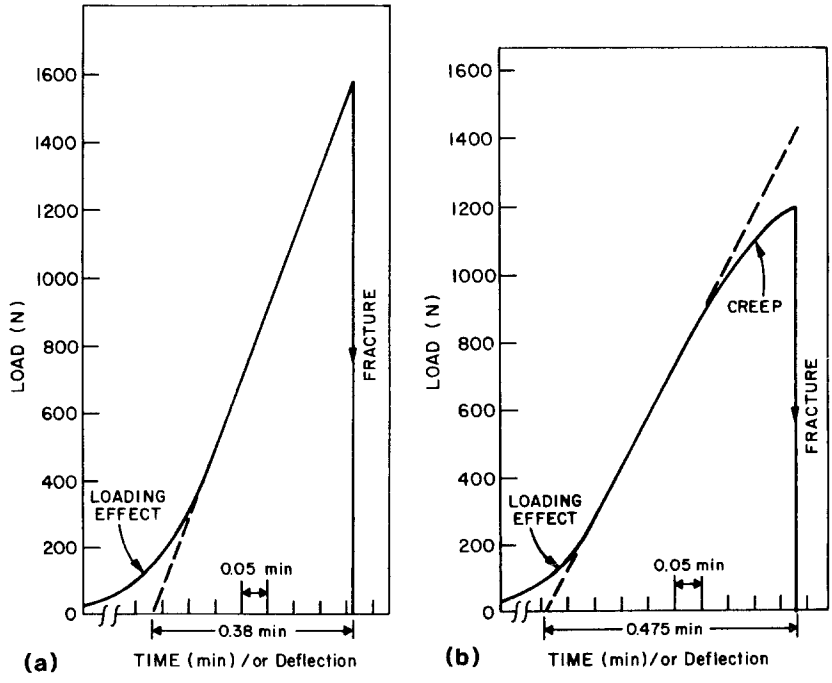

Figure 7 Typical traces of load–deflection curves for 85 wt % alumina + 15 wt % SiC whisker specimens tested in four-point bending in a fast fracture mode at (a) 1300° C and (b) 1400° C. Machine cross-head speed 0.5 mm min^{-1}. Note the deviation from the linear (elastic) portion of the curve at 1400° C due to extensive viscous flow (glass softening). Fracture surface for this specimen is shown in Fig. 8.

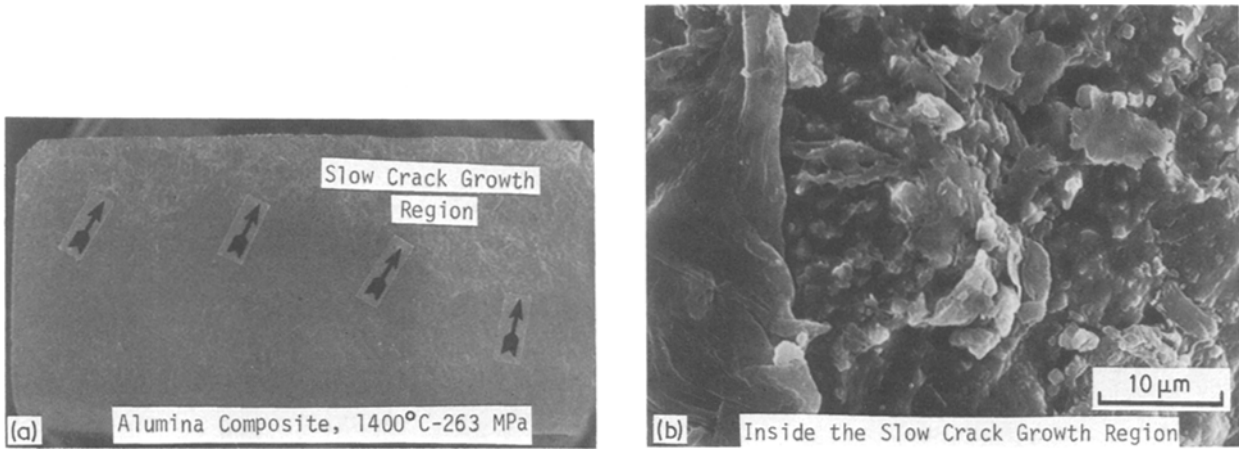

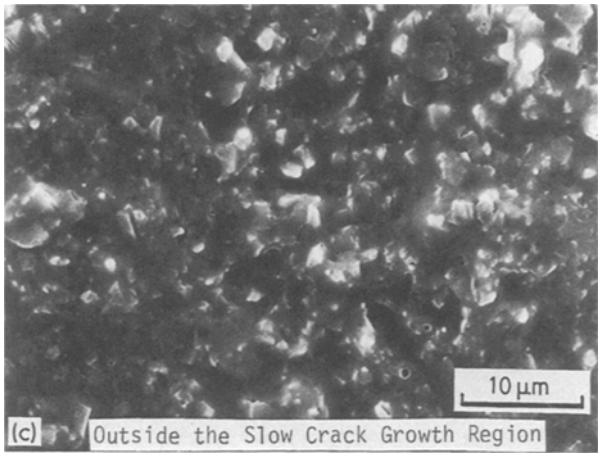

Figure 8 Typical fracture surface as seen in SEM for an alumina composite specimen tested in a fast fracture mode at 1400° C showing creep deformation.

and intergranular crack propagation, Fig. 8c. Note that the matrix grains, Fig. 8c, are smeared and the SiC-whiskers are no longer visible due to viscous glass formation. The large extent of viscous glass formation occurring at this temperature (1400° C) over the entire fracture surface becomes distinctly clear when the matrix microstructure are compared with tests carried out at lower temperatures, say 1000° C, Figs 8b, c and 6b, c, respectively.

The polycrystalline alumina behaved in a similar fashion as the alumina composite in the temperature range 1200 to 1400° C. In addition, the polycrystalline alumina was susceptible to porosity-related failures and extensive viscous glass formation at 1200° C (as shown in stress rupture results). Up to 1300° C, the fast fracture, load–deflection/time curves did not show signs of creep deformation. The majority of the failures occurred either at a surface porosity, Fig. 9, or at an "agglomerate or zone" of large-grained alumina grains, Figs 10 and 11, as the failure-initiating sources. The energy dispersive spectrometer analysis of these "agglomerates" revealed the presence of magnesium and yttrium as mentioned in the chemical composition. The origin of these large-grained alumina grains is not clearly understood. It is believed that the oxide additives (MgO and Y_2O_3 were not uniformly distributed in the alumina powder, and during hot-pressing promoted the formation of local liquid zones and upon cooling became the site for rapid or exaggerated grain growth. It should be pointed out that both these oxide additives also promote the formation of glassy phases whose presence was confirmed in stress rupture tests (see later). Recently, Dalgleish *et al.* [10],

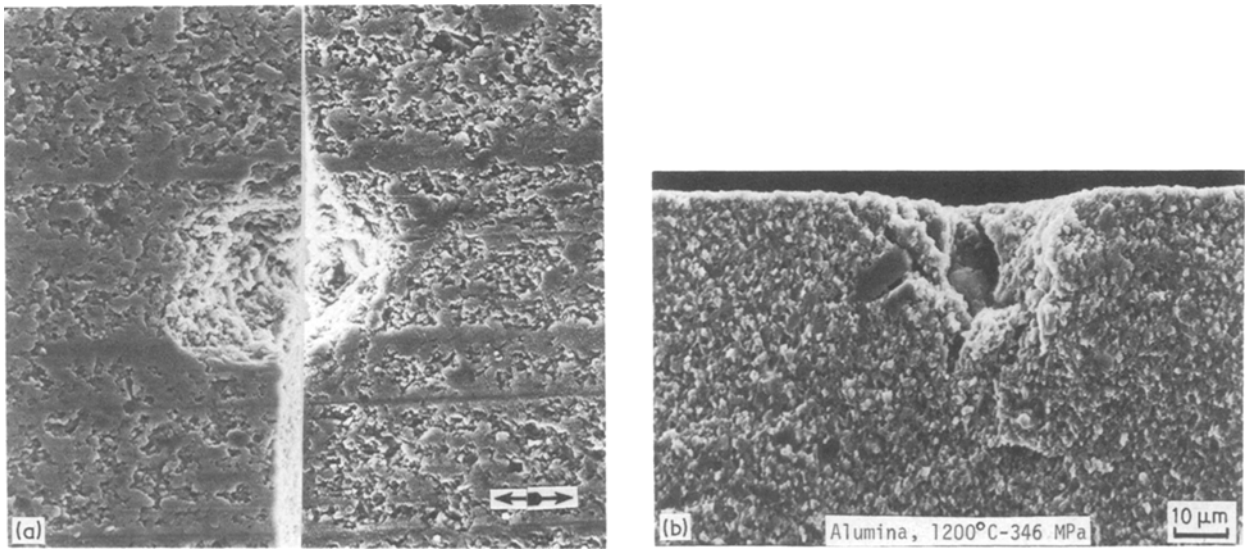

Figure 9 Scanning electron micrographs (same magnification) showing failure occurring at a surface porosity. (a) As-machined tensile surface of the specimen. Arrows indicate the machining direction. (b) Fracture surface. Note the presence of a large alumina grain.

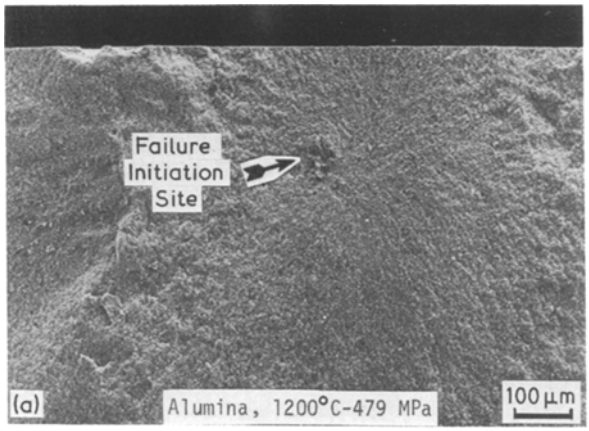

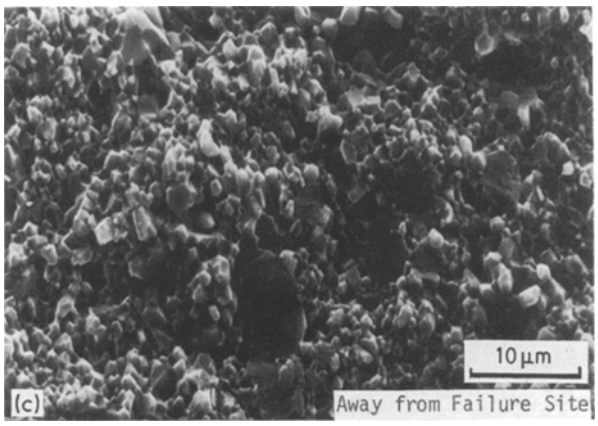

Figure 10 SEM fractographs showing sub-surface failure initiation at an "agglomerate" of large-grained alumina grains. Note the large alumina grains fractured transgranularly (cleaved) (b) while fine-grained matrix displayed intergranular failure (c).

Blumenthal and Evans [11] and Johnson *et al.* [12] studied the high-temperature (1300 to 1400° C) fracture of hot-pressed, large-grained polycrystalline alumina, and reported crack nucleation and large scale shear-band formation at chemical or microstructural heterogeneities similar to that reported in this study. The extensive shear band formation clearly suggests that their alumina matrix [10–12] contained large amounts of glassy phase. In the present study, no shear band formation or crack nucleation was observed on the tensile surface of test specimens of either polycrystalline alumina or alumina composite. In addition, the alumina composite did not show such large failure origins, Fig. 6, as observed in polycrystalline alumina, Figs 10 and 11, thereby suggesting that the presence of SiC whiskers may decrease or inhibit localized exaggerated grain growth. Similar views were expressed by Porter *et al.* [5] in a comparable material. In short, the alumina composite displayed significantly higher fracture strength relative to the polycrystalline alumina, especially in the temperature-independent region (20 to 800° C), Fig. 5. Above 800° C, both material showed decreasing strength due to creep deformation.

3.2. Flexural stress rupture

Flexural stress rupture tests were carried out as a function of temperature (600 to 1200° C) and applied stress in order to determine (i) the material's susceptibility for low-temperature instability, (ii) the presence of SCG at high temperatures (800 to 1200° C) and (iii) to identify allowable stress levels for limited time ($\leqslant$ 100 h) without showing any creep. A total of 36 specimens taken from both materials were tested in stress rupture mode and the results are summarized in Table III. For the polycrystalline alumina, at 600° C, two specimens were tested at an applied stress of 276 MPa and failed in 3 and 28 h. The test specimen failing in 3 h, failed at the loading edge of the test fixture and did not show clearly the failure initiation site. The other specimen failed at a sub-surface "zone of large alumina grains" similar to those seen in fast fracture mode at elevated temperatures, Figs 10 and 11. As the applied stress was increased to 344 MPa, the test specimen failed in 4 h. A typical fracture surface for this time-dependent failure is shown in Fig. 12, and clearly reveals that the failure was due to the presence

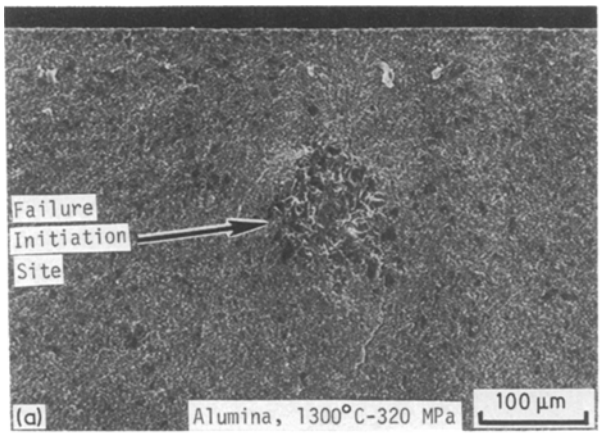

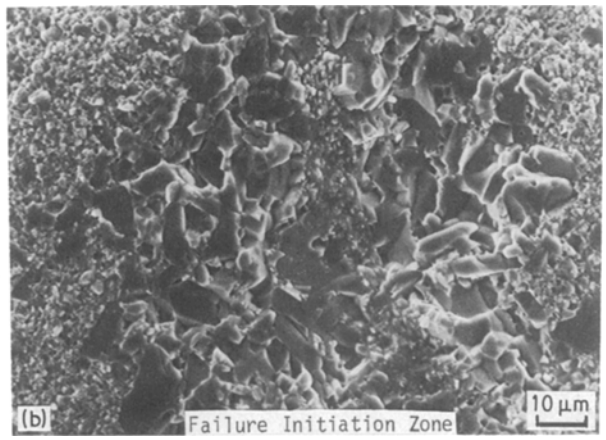

Figure 11 SEM fractographs showing failure initiation at an "agglomerate" of large-grained alumina grains.

TABLE III Flexural stress rupture results for hot-pressed alumina and alumina composite

Test temp. (°C)	Applied stress (MPa)	Failure time (h)	Sustained time without failure (h)	Remarks*
Alumina				
600	276	3	–	Specimen failed at the loading edge
600	276	28	–	SSF — Zone of large alumina grains
600	344	4	–	SF — Zone of large alumina grains, Fig. 12
800	276	–	287	No discolouration, no bending
800	344	0	–	Failed instantly
800	344	6	–	Specimen failed in multiple pieces
800	344	37	–	Specimen failed in multiple pieces
800	344	355	–	Specimen failed in multiple pieces
800	413	0	–	Failed instantly
800	413	0	–	Failed instantly
800	413	418	–	Specimen failed at the loading edge
1000	344	216	–	Specimen failed at the loading edge
1000	344	–	305	No discolouration, no bending
1000	344	–	214	No discolouration, no bending
1000	413	0	–	Failed instantly
1200	207	–	42	Specimen displayed bending, Fig. 13
1200	276	–	70	Specimen displayed extensive bending
Alumina composite				
600	276	–	150	No discolouration, no bending
800	413	–	312	No discolouration, no bending
800	413	–	310	No discolouration, no bending
800	413	–	360	No discolouration, no bending
1000	344	0	–	Failed instantly
1000	344	–	235	No discolouration, no bending
1000	344	–	310	No discolouration, no bending
1000	344	–	503	No discolouration, no bending
1000	413	0.016	–	SF and SSF
1000	413	0.016	–	SF
1000	413	59	–	SSF — Zone of large alumina grains
1000	413	352	–	SF and SSF, large alumina grains
1000	413	–	218	No discolouration, no bending
1200	207	1.5	–	Limited SCG
1200	207	3.3	–	SCG, Fig. 14
1200	207	23	–	SCG
1200	276	0.6	–	Limited SCG
1200	344	0.1	–	Limited SCG
1200	344	0.1	–	Limited SCG

*SF = surface flaw; SSF = sub-surface flaw; SCG = slow crack growth.

of a "zone of large alumina grains". At this low temperature (600° C) of testing, the fracture surface did not show the presence of SCG indicative of glass formation.

Increasing the temperature to 800 and 1000° C did not significantly change the fracture behaviour of the material. At 800° C and 413 MPa, three specimens were tested. Two failed instantly and the third specimen failed after 418 h at the loading edge of the test fixture. As the applied stress was decreased to 344 MPa, four specimens were tested, one failed instantly and the other three failed in periods ranging from 6 to 355 h. At 1000° C and 413 MPa, one specimen was tested and failed instantly. As the applied stress was decreased to 344 MPa, three specimens were tested, one failed in 216 h and the other two sustained the stress for over 200 h without failure.

At 1200° C, the material showed a distinctly different behaviour than that seen at 800 and 1000° C. The material was incapable of sustaining even low stress levels of 207 MPa and displayed significant bending in short duration (42 h), Fig. 13, suggesting the onset of viscous flow or residual glass softening. This macroscopic bending of the specimen clearly points out the importance of this temperature and applied stress (1200° C and 207 MPa) for the onset of grain-boundary sliding as a creep mechanism.

The SiC-whisker-reinforced alumina composite showed a slightly better performance than that shown by the polycrystalline alumina in the temperature-independent region (20 to 800° C). At 800° C and at an applied stress level of 413 MPa, three specimens were tested, all sustained over 300 h without failure and did not show any visible signs of degradation such as surface cracking or bending. At 1000° C and 344 MPa, four specimens were tested, one failed instantly and three sustained the stress for over 200 h without failure and bending. As the applied stress was increased to

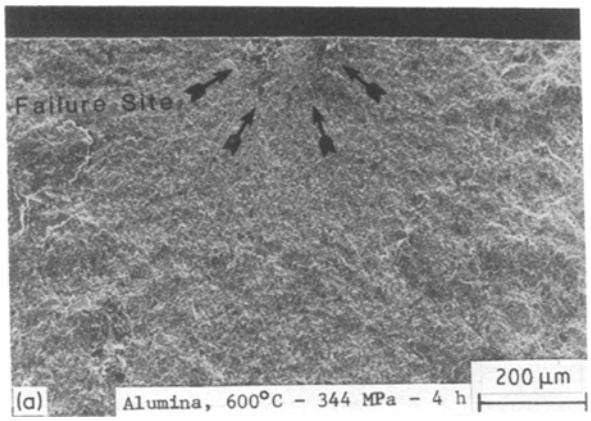

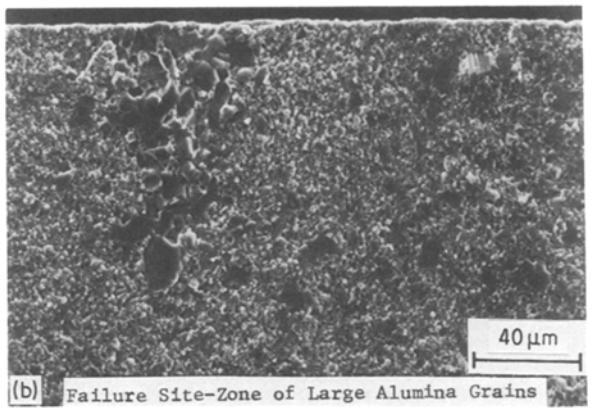

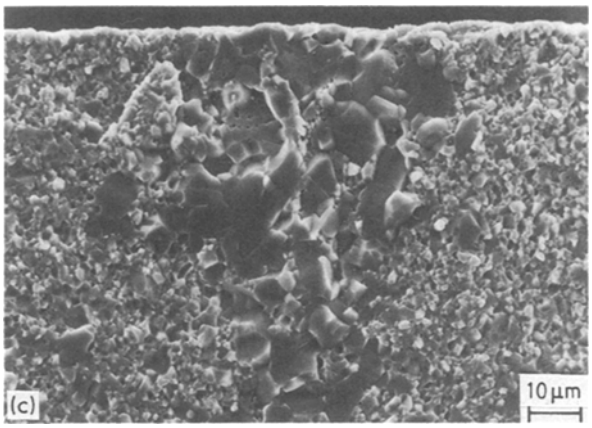

Figure 12 SEM fractographs showing failure initiation site. The presence of a processing defect (zone of large alumina grains) led to early failure at a relatively low applied stress and temperature.

413 MPa, five specimens were tested, two failed almost instantly (0.016 h), two failed after 59 and 352 h and one sustained over 200 h without showing any signs of bending. It is important to note that specimens of both materials (alumina and alumina composite) displayed instant failures at relatively low applied stresses and temperatures, such as 344 to 413 MPa and 800 to 1000° C, respectively, and displayed failures originating at an "agglomerate" of large alumina grains. These are primarily processing defects and can be eliminated or reduced by choosing proper hot-pressing or sintering conditions such as time, temperature, environment and pressure.

At 1200° C and 207 MPa, the alumina composite showed a distinctly different behaviour than that seen up to 1000° C. Three specimens were tested and failed in 1.5, 3.3 and 23 h. All of them displayed the presence of SCG. A typical fracture surface for the specimen failing in 3.3 h is shown in Fig. 14, revealing a large region of SCG, Fig. 14a, and extensive viscous flow due to glass formation causing smearing of grains, cavity and crack formation, Fig. 14b. This fracture surface (Fig. 14a) has a lot of similarities to that seen in fast fracture mode, Fig. 8, and tested at a significantly higher temperature of 1400° C. The remainder of the fracture surface, Fig. 14c, displayed much less glass smearing effect, the SiC-whisker distribution in the alumina matrix and whisker pull-out are clearly visible. Stress rupture testing at 1200° C for both materials clearly pointed out the importance of such testing compared to most commonly used fast fracture testing, Fig. 5. At 1200° C and 207 MPa, for polycrystalline alumina, bending of the specimen, Fig. 13, and for the alumina composite, failure occurring in a short time and showing SCG, could not have been detected or predicted from fast fracture testing, Fig. 5. As the applied stress was increased to 276 and 344 MPa, failure occurred rapidly (0.6 to 0.1 h).

4. Conclusion

The 15 wt % SiC-whisker-reinforced alumina composite displayed significantly higher fracture strength and toughness at 20° C compared to polycrystalline alumina. For both materials, σ_F was independent of temperature from 20 to 800° C. Above 800° C, σ_F, decreased with increasing temperature due to the presence of SCG. At 1200° C and above, both materials showed degradation of strength due to creep deformation.

Both materials contained large-size processing defects such as "agglomerates of large-grained alumina", which led to instant failures in flexural stress rupture testing at applied stress levels of 344 and 413 MPa and at temperatures of 800 and 1000° C. Therefore, it is suggested that these materials should not be subjected to stresses over 200 MPa at temperatures up to 1000° C. Above 1000° C, the materials are unstable and show creep deformation.

Acknowledgements

The author thanks R. Goss for scanning electron microscopy work and Dr T. J. Whalen for suggesting the study and critically reading the paper. Thanks are also due to Dr J. F. Rhodes for supplying hot-pressed alumina and alumina composite.

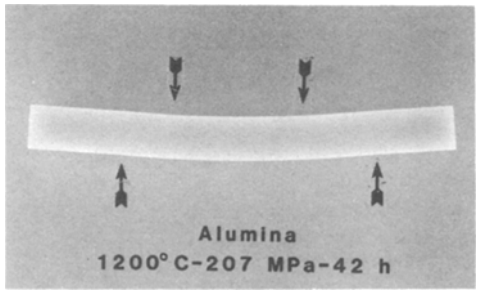

Figure 13 Overall view of the flexural specimen of alumina showing extensive bending. Arrows indicate approximate positions of inner and outer loading edges.

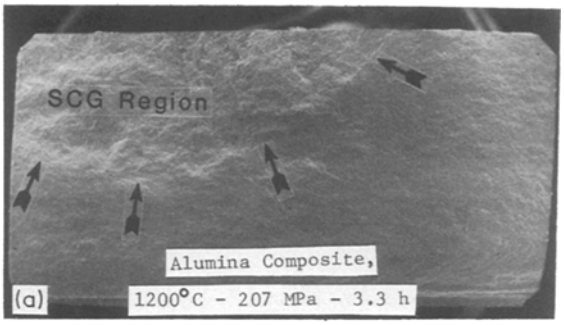

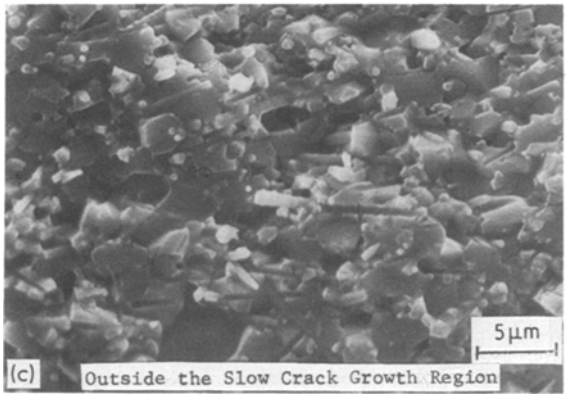

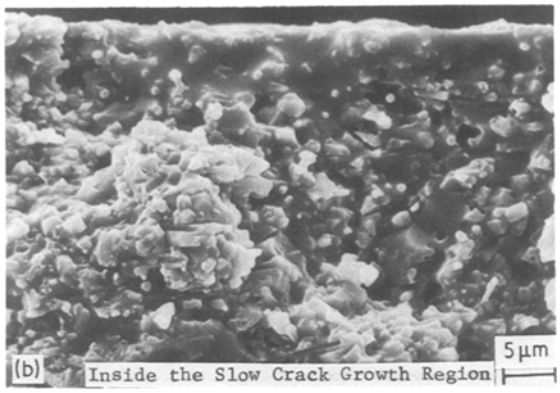

Figure 14 Typical fracture surface as seen in SEM for a specimen tested in stress rupture mode.

References

1. I. W. DONALD and P. W. McMILLAN, *J. Mater. Sci.* **11** (1976) 949.
2. P. F. BECHER and G. C. WEI, *J. Amer. Ceram. Soc.* **67** (1984) C-267.
3. G. C. WEI and P. F. BECHER, *Amer. Ceram. Soc. Bull.* **64** (1985) 298.
4. J. HOMENY, W. L. VAUGHN and M. K. FERBER, *ibid.* **66** (1987) 333.
5. J. R. PORTER, F. F. LANGE and A. H. CHOKSHI, *ibid.* **66** (1987) 343.
6. R. K. GOVILA, "Ceramic Life Prediction Parameters", Tech. Rept. TR 80-18, Army Materials and Mechanics Research Center, Watertown, Massachusetts 02172 (May 1980).
7. *Idem, J. Mater. Sci.* **20** (1985) 4345.
8. *Idem, Amer. Ceram. Soc. Bull.* **65** (1986) 1287.
9. A. G. EVANS and E. A. CHARLES, *J. Amer. Ceram. Soc.* **59** (1976) 371.
10. B. J. DALGLEISH, S. M. JOHNSON and A. G. EVANS, *ibid.* **67** (1984) 741.
11. W. BLUMENTHAL and A. G. EVANS, *ibid.* **67** (1984) 751.
12. S. M. JOHNSON, B. J. DALGLEISH and A. G. EVANS, *ibid.* **67** (1984) 759.

Received 8 October 1987
and accepted 29 January 1988